J. Basic. Appl. Sci. Res., 2(6)5478-5486, 2012

ISSN 2090-4304
Journal of Basic and Applied Scientific Research
www.textroad.com

An Optimized Ride through Protection Method for DFIG Wind Turbine during Asymmetrical Disturbance

Alireza Zohoori[1], Rouhollah Shafaie[1]

[1]The Center of Excellence for Power System Automation and Operation, Department of Electrical Engineering
Iran University of Science and Technology, Tehran, Iran

ABSTRACT

In this paper a complete analysis for calculating the stator flux vector of the doubly fed induction generator (DFIG) under symmetrical and asymmetrical network disturbances was performed without neglecting neither the stator resistance nor the slip frequency. The effect of different fault occurrence time on the amplitude of the stator current is then investigated. Consequently, an optimal crowbar resistance for fault ride through protection of DFIG under network disturbance is proposed by employing the mathematical algorithm of Analytic Hierarchy Process (AHP). A typical relative importance is selected and optimization is carried out. Simulation results for an optimized crowbar demonstrated that the proposed protection control system can improve the stator voltage during the fault and the faster retrieval after the fault.
Keywords: Doubly Fed Induction Generator; Crowbar Optimization; Reactive power; Analytic Hierarchy Process;Voltage disturbance.

1. INTRODUCTION

Recently the number of variable speed wind turbines connected to the grid, especially those using doubly fed induction generator (DFIG), is constantly increasing. The most significant advantage of this kind of turbines emerges in the rating of their converter which is around 25–35% of the turbine rated power. Moreover not only cost, size and weight collaborated with a small converter are lower but also losses are smaller than the wind turbines based on full power converters connected to the stator [1]. Since the stator is directly connected to the gird as shown in Fig.1, these types of wind turbines are so much sensitive to network disturbances especially fault conditions which become the main problem.

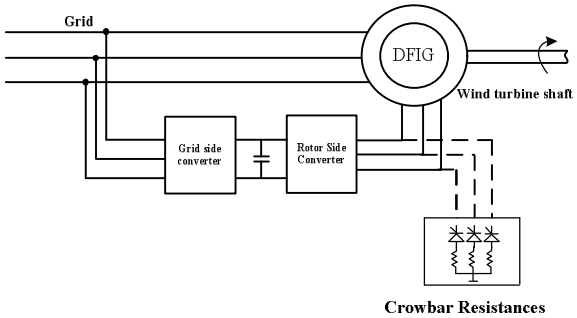

Fig. 1. Schematic of DFIG wind turbine connected to the grid

A sudden grid voltage drop because of network disturbance, that are mainly symmetrical or asymmetrical faults, create over-voltages and over-currents in the rotor windings that can destroy the rotor side converter (RSC) if no proper protection method is considered [2]. The protection method to deal with the problems and improve fault ride through (FRT) capability is concealed in connecting rotor winding to the crowbar resistors [3, 4, 5]. The crowbar must limit the rotor current in a way that rotor terminal voltage does not exceed from the rated voltage. This means that smaller the crowbar the better it is [4, 6].From another point of view, a larger crowbar resistance to limit the rotor peak current is more desirable [4, 6]. Hence, one of the best and most common methods for FRT control system is selecting the optimal crowbar resistors. The crowbar value must be chosen in the way that not only provide FRT capability of the DFIG but also guarantee fast wind turbine restoration. Crowbar optimization method was partially discussed in [4, 5, 6, 7], where in most of them the optimization performed either by the iterative manner or shallow one just for symmetrical three phase fault. Theoretical method in finding an optimal crowbar was partially discussed in [8] for a single phase fault.

In this paper the authors develop the idea for all type of network fault condition based on analytical hierarchy process (AHP). Accordingly, the optimal crowbar is obtained. Beside, thorough analysis for calculating the stator flux vector of the DFIG under symmetrical and asymmetrical network disturbances is performed without neglecting neither the stator resistance nor the slip frequency which were not considered in later studies [4,5,6]. Simulation results prove that the proposed protection system can provide a high desirable FRT performance of the DFIG during network disturbances.

Corresponding Author : Alireza Zohoori, The Center of Excellence for Power System Automation and Operation, Department of Electrical Engineering, Iran University of Science and Technology, Tehran, Iran.
Email: alirezazohouri@iust.ac.ir

2. DFIGBehavior Under Network Disturbance

In this section the proposed method for stator flux vector calculation is obtained for asymmetrical fault condition. Notice that for symmetrical fault the same equations are applied by neglecting the negative sequence of the stator voltage vector in all the equations.

For simplifying the study, the rotor variables will be referred to the stator. Here d-q references frame rotating at synchronous speed ω_s is used by [6]:

$$\begin{pmatrix} v_{ds} \\ v_{qs} \end{pmatrix} = \begin{pmatrix} R_s & 0 \\ 0 & R_s \end{pmatrix} \begin{pmatrix} i_{ds} \\ i_{qs} \end{pmatrix} + d/dt \begin{pmatrix} \psi_{ds} \\ \psi_{qs} \end{pmatrix} + \begin{pmatrix} 0 & -\omega_s \\ \omega_s & 0 \end{pmatrix} \begin{pmatrix} \psi_{ds} \\ \psi_{qs} \end{pmatrix} \tag{1}$$

$$\begin{pmatrix} v_{dr} \\ v_{qr} \end{pmatrix} = \begin{pmatrix} R_r & 0 \\ 0 & R_r \end{pmatrix} \begin{pmatrix} i_{dr} \\ i_{qr} \end{pmatrix} + d/dt \begin{pmatrix} \psi_{dr} \\ \psi_{qr} \end{pmatrix} + \begin{pmatrix} 0 & -s\omega_s \\ s\omega_s & 0 \end{pmatrix} \begin{pmatrix} \psi_{dr} \\ \psi_{qr} \end{pmatrix} \tag{2}$$

Since the stator is connected to the grid directly, the grid impose the stator voltages v_{ds} and v_{qs}. The rotor voltage v_{qr} and v_{dr} are forced by a RSC which controls the machine performance. The stator and rotor flux of the d-q axis can be reached by [6]:

$$\begin{pmatrix} \psi_{ds} \\ \psi_{dr} \end{pmatrix} = \begin{pmatrix} L_s & L_m \\ L_m & L_r \end{pmatrix} \begin{pmatrix} i_{ds} \\ i_{dr} \end{pmatrix} \tag{3}$$

$$\begin{pmatrix} \psi_{qs} \\ \psi_{qr} \end{pmatrix} = \begin{pmatrix} L_s & L_m \\ L_m & L_r \end{pmatrix} \begin{pmatrix} i_{qs} \\ i_{qr} \end{pmatrix} \tag{4}$$

where L_s and L_r are the stator and rotor inductance, respectively and L_m is the magnetizing inductance.

Inversing (3) and (4) then substituting in (1) and (2) given the following equation [7]:

$$\begin{pmatrix} v^+_{ds} \\ v^+_{qs} \\ v^+_{dr} \\ v^+_{qr} \end{pmatrix} = \begin{pmatrix} R_s/L_{sz} & -\omega_s & -R_s L_m/L_s L_{rz} & 0 \\ \omega_s & R_s/L_{sz} & 0 & -R_s L_m/L_s L_{rz} \\ -R_r L_m/L_r L_{sz} & 0 & R_r/L_{rz} & -s\omega_s \\ 0 & -R_r L_m/L_r L_{sz} & s\omega_s & R_r/L_{rz} \end{pmatrix} \begin{pmatrix} \psi^+_{ds} \\ \psi^+_{qs} \\ \psi^+_{dr} \\ \psi^+_{qr} \end{pmatrix} \tag{5}$$

$$\begin{pmatrix} v^-_{ds} \\ v^-_{qs} \\ v^-_{dr} \\ v^-_{qr} \end{pmatrix} = \begin{pmatrix} R_s/L_{sz} & 1 & -R_s L_m/L_s L_{rz} & 0 \\ -1 & R_s/L_{sz} & 0 & -R_s L_m/L_s L_{rz} \\ -R_r L_m/L_r L_{sz} & 0 & R_r/L_{rz} & -(\omega_s+\omega) \\ 0 & -R_r L_m/L_r L_{sz} & \omega_s+\omega & R_r/L_{rz} \end{pmatrix} \begin{pmatrix} \psi^-_{ds} \\ \psi^-_{qs} \\ \psi^-_{dr} \\ \psi^-_{qr} \end{pmatrix} \tag{6}$$

where L_{rz} and L_{sz} are given as:

$$L_{rz} = L_r - (L^2_m/L_s) \tag{7}$$

$$L_{sz} = L_s - (L^2_m/L_r) \tag{8}$$

The effect of asymmetrical faults in phase voltages can be studied according to symmetrical components theory. Based on this theory, a three phase voltage system can be expressed as the sum of three components: positive, negative, and zero sequences. Therefore the stator voltage space vector can be decomposed into three vectors:

$$\vec{v}_s = \vec{v}_1 e^{j\omega_s t} + \vec{v}_2 e^{-j\omega_s t} + \vec{v}_0 \tag{9}$$

For a given classical machine with symmetrical impedances, the positive sequence $\vec{v}_1$ creates a flux rotating at the synchronous speed and the negative sequence $\vec{v}_2$ creates a flux rotating with magnitude of the synchronous speed but in the opposite direction. Also, the zero sequence $\vec{v}_0$ does not create any flux. These voltages create forced and natural flux respectively which is fully discussed in [4].

Now different kind of fault condition will be investigated through the following subsections.

A. *Single-Phase Faults*

A single phase fault drops the voltage. Taking into account equal impedance for the positive and the negative sequence, the positive, negative and zero components expressed as:

$$\begin{bmatrix} \vec{V}_1 \\ \vec{V}_2 \\ \vec{V}_3 \end{bmatrix} = 1/3 \begin{bmatrix} 1 & \vec{a} & \vec{a}^2 \\ 1 & \vec{a}^2 & \vec{a} \\ 1 & 1 & 1 \end{bmatrix} . \begin{bmatrix} V(1-p) \\ V.\vec{a}^2 \\ V.\vec{a} \end{bmatrix} = v . \begin{bmatrix} 1-p/3 \\ -p/3 \\ -p/3 \end{bmatrix} \tag{11}$$

The stator flux vector after the fault occurrence can be obtained from (5), (6) and (10) in d-q synchronous frame as:

$$\vec{\psi}_{ds}^{af} = \vec{\psi}_{ds}^{+} + \vec{\psi}_{ds}^{-}.e^{-2j\omega_s t_2} + \left[\left(\vec{\psi}_{ds}^{bf} - \left(\vec{\psi}_{ds}^{+} + \vec{\psi}_{\bar{ds}}.e^{-2j\omega_s t_1}\right)\right).e^{-\omega_s t_2/\tau_s}.e^{-2j\omega_s t_2}\right] \quad (11)$$

$$\vec{\psi}_{qs}^{af} = \vec{\psi}_{qs}^{+} + \vec{\psi}_{qs}^{-}.e^{-2j\omega_s t_2} + \left[\left(\vec{\psi}_{qs}^{bf} - \left(\vec{\psi}_{qs}^{+} + \vec{\psi}_{qs}^{-}.e^{-2j\omega_s t_1}\right)\right).e^{-\omega_s t_2/\tau_s}.e^{-2j\omega_s t_2}\right] \quad (12)$$

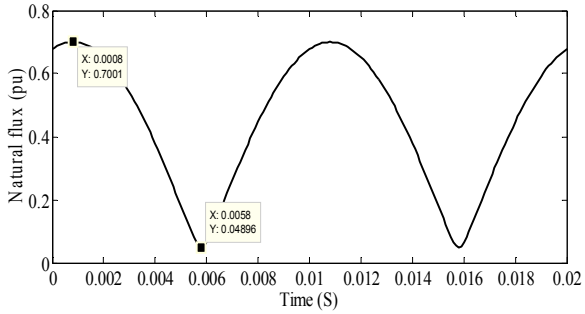

Fig. 2. Natraul flux value for different time of single phase fault

Where t_1 and t_2 are the time just before and after the fault occurrence respectively. $\vec{\psi}_{ds}^{af}$ And $\vec{\psi}_{ds}^{bf}$ are the stator flux vectors after and before fault occurrence, respectively. Note that the stator flux vector is obtained without neglecting neither the stator resistance nor the slip frequency. The second part of the (11) and (12), the terms in brackets, are explaining the natural flux. It is obvious that with different time of fault occurrence the natural flux is changing from a minimum value to a maximum value, so it affects on total preliminary stator flux vector hence the amplitude of the stator current change based on this flux values. Fig. 2 shows the natural flux variation for different time of single phase faults in a specific generator that the machine parameters are given in Appendix. According to Fig. 2 the natural flux domain are obtained as:

$$y_{sn}(\max) = 0.7001$$
$$y_{sn}(\min) = 0.04896 \quad (13)$$

The effect of obtained natural flux values on the stator current amplitude can be seen in Fig. 3 and Fig. 4. Beside, the stator flux trajectory before and after the fault occurrence is demonstrated in Fig. 5.

B. Phase to phase fault

The positive, negative, and zero voltage components are as follows [3]:

$$\begin{bmatrix}\vec{V}_1\\ \vec{V}_2\\ \vec{V}_3\end{bmatrix} = v.\begin{bmatrix}1-p/2\\ p/2\\ p/2\end{bmatrix} \quad (14)$$

With the voltages shown in (14), the components of the stator flux vectors can be calculated from (11) and (12) as the latter. Fig. 6 shows the natural flux variation for different time of phase to phase faults in the model. According to Fig. 6 the natural flux amplitude are obtained as:

$$y_{sn}(\max) = 1.06$$
$$y_{sn}(\min) = 0.06426$$

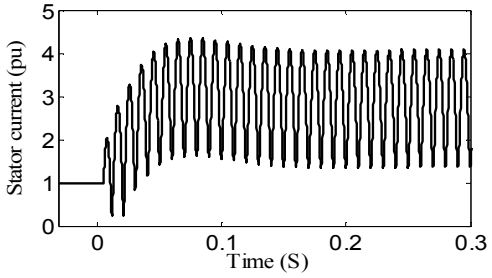

Fig. 4. Stator current variation under single phase for min natural flux

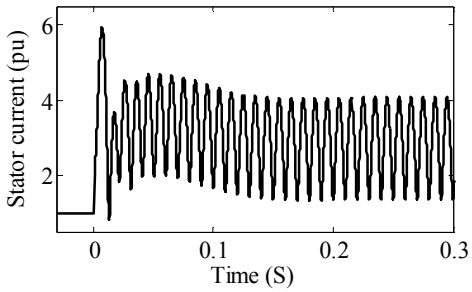

Fig. 3. Stator current variation under single phase fault for max natural flux

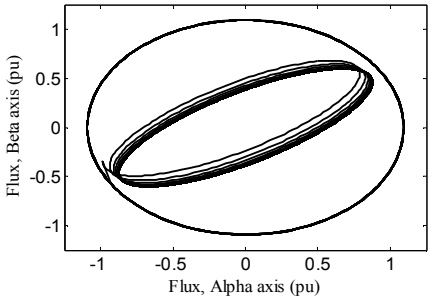

Fig. 5. Stator flux trajectory during single phase fault

The effect of achieved natural flux values on the stator current amplitude can be seen in Fig. 7 and Fig. 8. Fig.7 shows that the phase to phase fault has a magnitude of about 10 p.u on the rotor winding as well as the rotor side converter. This is because of the higher natural flux in two phase fault that is obtained in (15).Therefore it will destroy the GSC and RSC components if protection methods are not applied to the system.

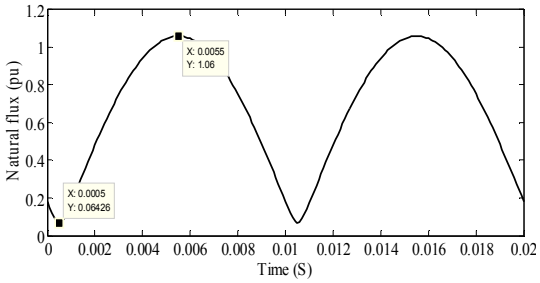

Fig. 6. Natraul flux value for different time of two phase fault

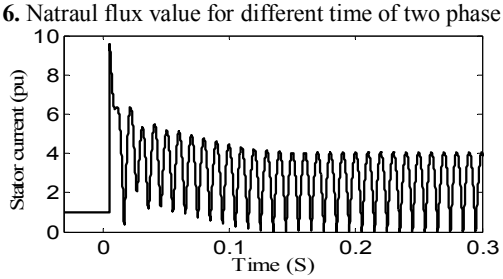

Fig. 7. Stator current variationunder phase to phase fault for max natural flux

Also, the stator flux trajectory before and after the fault occurrence is demonstrated in Fig. 9.

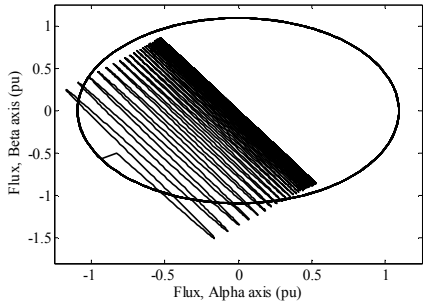

Fig. 9. Stator flux trajectory during phase to phase fault starts at $t_0 = 0$

3. CROWBAR OPTIMIZATION

The concept of the pair wise comparison is originated from psychological research that becomes the base of AHP. The AHP is used in the multiple criteria decision making applications. The decision maker in this method expresses linguistic pair wise comparison, at first; then, obtains numerical pair wise comparisons by selecting certain numerical scale to quantify them and eventually calculates priority vector from the numerical pair wise comparison [9].

The objective function of the present method is defined as below [9]:

$$F = w_1 I_r + w_2 T_e + w_3 V_r + w_4 Q_s \quad (16)$$

Where w_1, w_2, w_3 and w_4 are relative importance of normalized constraints of rotor current I_r, electromagnetic torque T_e, rotor voltage V_r and reactive power Q_s, respectively. Note that these parameters are obtained by simulation of DFIG under network disturbances with different crowbar resistance values. It should be mention that these quantities are in different ranges so the constraints are normalized to the interval of 1-9.

$$y_{normal} = \frac{d - c}{b - a}(x - a) + c \quad (17)$$

Fig. (17-a) and (17-b) refer to minimum and maximum peak values of obtained parameters from simulation, respectively and x is the value within this interval. Besides, c and d are equaled to one and nine, respectively. Moreover, the weights are calculated by AHP algorithm with respect to the fact that preferences are selected according to importance of variables. For instance, the preference of rotor terminal voltage is more than rotor current and electrical torque in order to protect the power electronic converter in terms of thermal insulation. After calculation of the weights, the objective function is plotted where the minimum point is an optimized crowbar for perfect DFIG performance during the fault considering less power absorption to have a better dynamic for faster voltage recovery after the fault .

In order to have a precise analysis of the effect of crowbar values on reactive power, rotor current, voltage and electrical torque for finding an optimize crowbar this paper used a fifth order algebraic differential equation of DFIG [10]. Here the optimized crowbar resistances for network disturbance for single phase, phase to phase and three phase network fault are shown in Fig. 10, Fig. 11 and Fig. 12, respectively. According to these figures, the optimized crowbar values are obtained as 0.34 p.u., 0.3 p.u. and 0.24 p.u for single phase fault and phase to phase fault, respectively.

4. EVALUATION OF THE PROTECTION CONTROL SYSTEM

In this section simulation is carried out for different crowbar values for symmetrical and asymmetrical network fault condition. Notice that network disturbances occurred at time 10.0021s. As we can see in these figures the optimized crowbar satisfies the constraints.

As pointed out in fig.7 and fig.8 the lower value for crowbar causes the larger peak current and electrical torque. As shown fig.9 an increment in crowbar results higher rotor terminal voltage during fault.

A- Symmetrical Fault

Figure 13 shows the stator current amplitude variation under three phase fault for two crowbar resistance that one is the optimized crowbar achieved in the last section. Also, Fig. 15 is demonstrating the torque and active power of the generator during the same condition. As pointed out in Fig. 13 and Fig. 14 the lower value for crowbar causes the larger peak current and electrical torque amplitude.

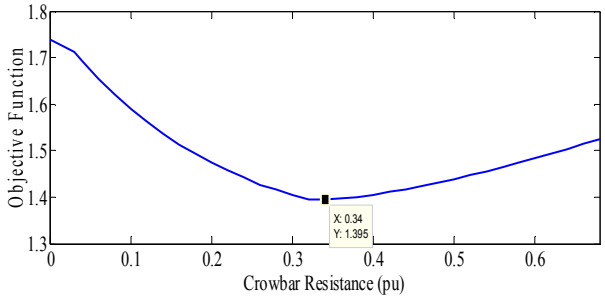

Fig. 10. Objective function versus crowbar under single phase fault

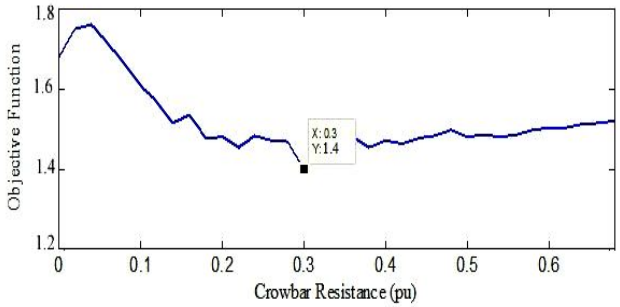

Fig. 11. Objective function versus crowbar under 2 phase fault

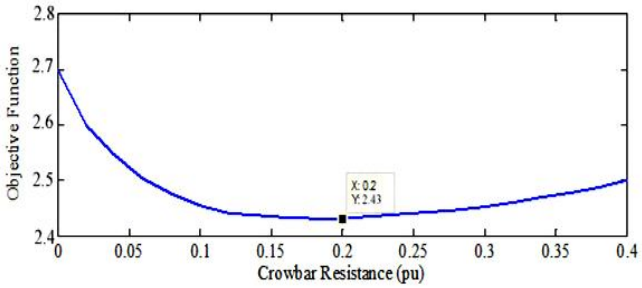

Fig. 12. Objective function versus crowbar under three phase fault

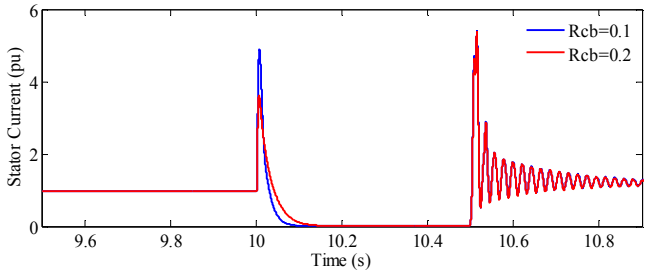

Fig. 13. Stator Current amplitude variation during symmetrical fault

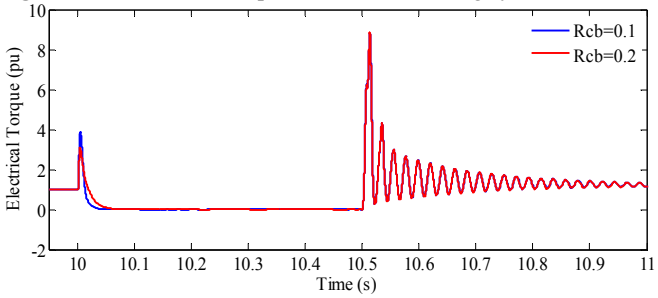

Fig. 14. Electrical torque variation during symmetrical fault

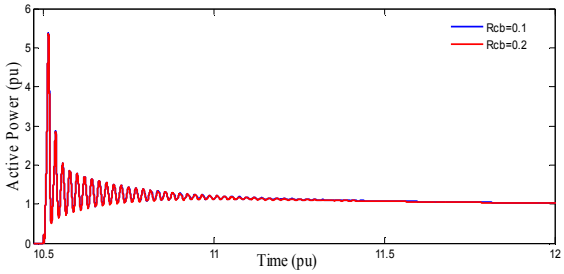

Fig. 15. Active power variation during symmetrical fault

B- Asymmetrical Fault

Figure 16 shows the stator current amplitude variation for optimized and non-optimized crowbar resistance under single phase fault. Also, Fig. 17, Fig. 18 and Fig. 19 are presenting the torque, active and reactive power of the DFIG during the same condition.

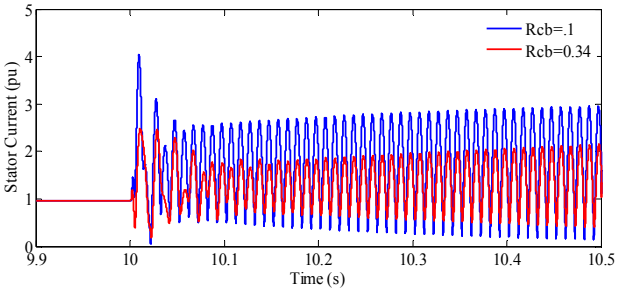

Fig. 16. Stator current amplitude variation during single phase fault

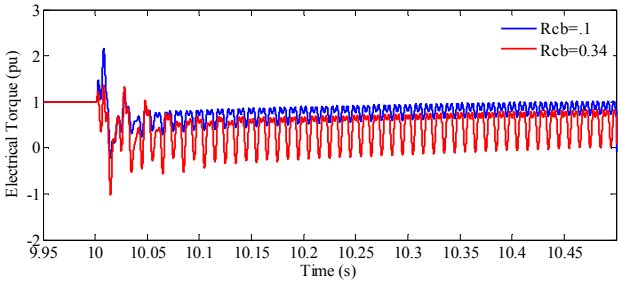

Fig. 17. Electrical torque variation during single phase fault

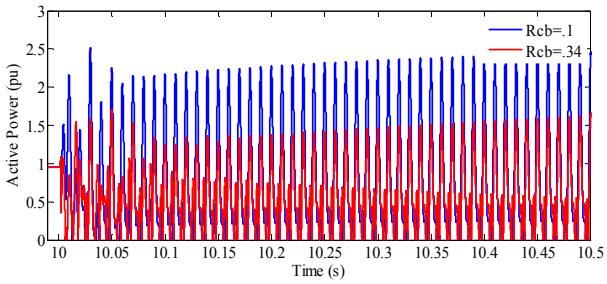

Fig 18. Active power variation during single phase fault

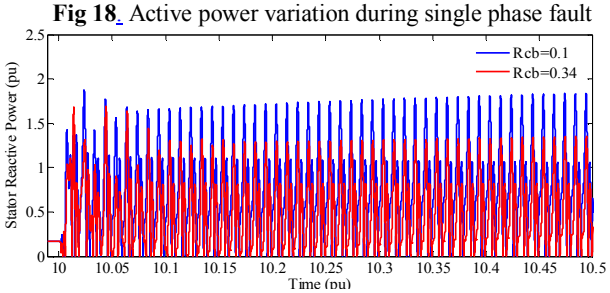

Fig. 19. Reactive power variation during single phase fault

In the same manner the similar figures are obtained for phase to phase fault condition with optimized crowbar protection control system that can be seen in Fig. 20 to Fig. 23.

As it is shown in Fig. 19 and Fig. 23 the better ride through protection control system is obtained by the proposed crowbar optimization method.

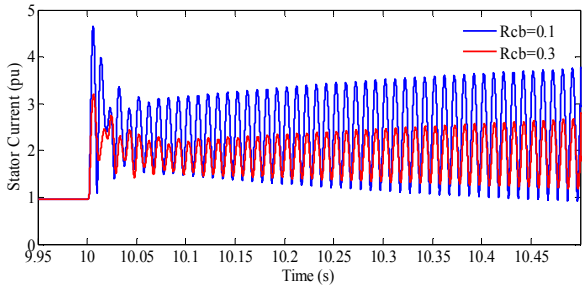

Fig. 20. Stator current amplitude variation during phase to phase fault

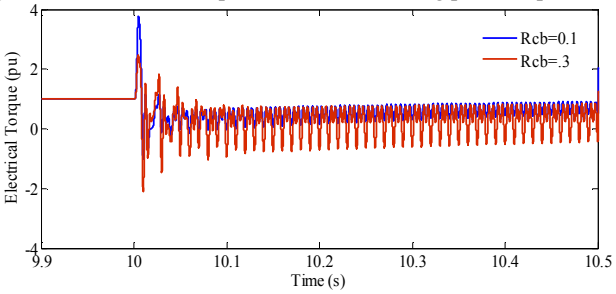

Fig. 21. Electrical torque variation during phase to phase fault

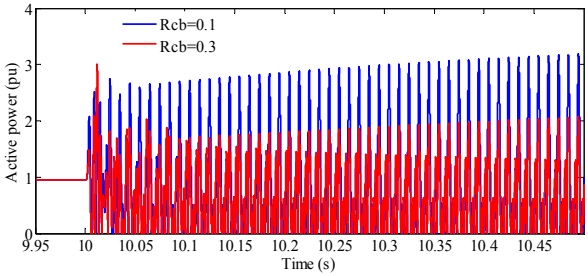

Fig. 22. Active power variation during phase to phase fault

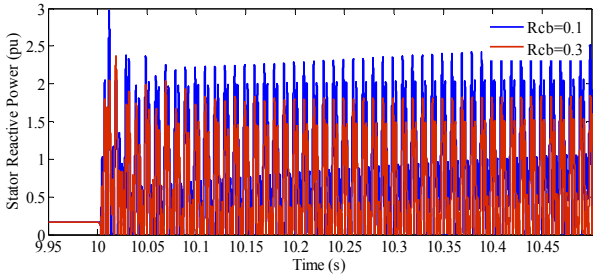

Fig. 23. Reactive power variation during phase to phase fault

1. CASE STUDY FOR TYPICAL GRID

The obtained optimized crowbar during network disturbances are applied to a typical grid as it is shown in Fig. 24. The stator voltage amplitude variations during symmetrical and asymmetrical network disturbances are shown in Fig. 25 to Fig. 27, respectively. Also, results are obtained with different crowbar values. It is shown that the optimized crowbar will improve the DFIG FRT capability and provide faster restoration responses consequently enhanced the dynamic performance of wind turbine after the network disturbance. It can be seen that for a symmetrical fault changes in amplitude of stator voltage is less than two other types of asymmetrical faults which are studied in this paper.

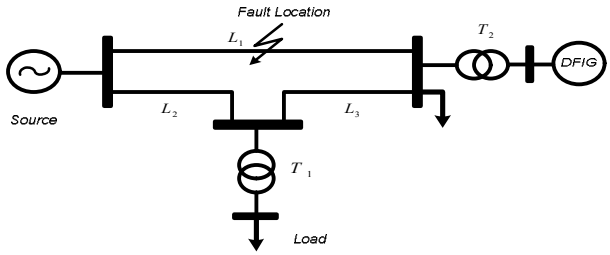

Fig. 24. Schematic of a typical grid

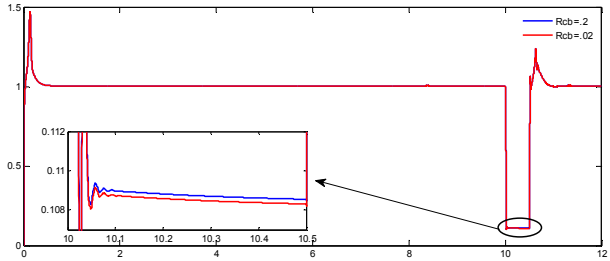

Fig. 25. Stator voltage amplitude variation during symmetrical grid fault

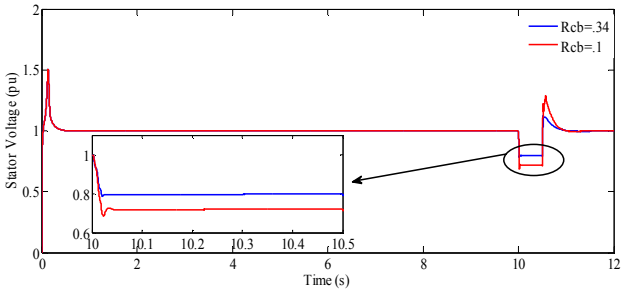

Fig. 26. Stator voltage amplitude variation during single phase grid fault

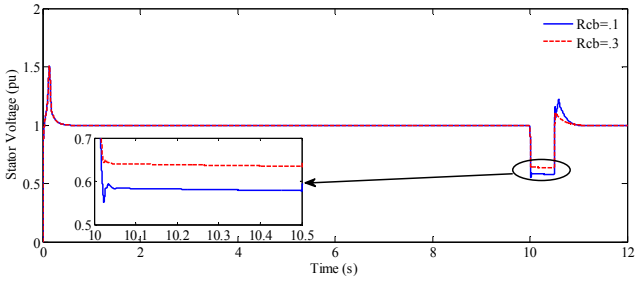

Fig. 27. Stator voltage amplitude variation during phase to phase grid fault

6. CONCLUSION

This paper is focused on comprehensive analysis to calculate the stator flux vector of DFIG under symmetrical and asymmetrical network disturbances. It is imperative that the proposed analysis is carried out by considering both the stator resistance and the slip frequency. The effect of different fault occurrence time on the amplitude of the stator current is then investigated. Moreover, an optimal crowbar resistance for FRT protection of DFIG under different kind of network distortion is proposed by applying the AHP method. Simulation results prove that the novel protection control system can provide a high desirable FRT performance and enhanced dynamic behavior of the DFIG during network disturbances.

APPENDIX

DFIG data	
p	2 MW
v_s	690 v
r_s	0.048 pu
r_r	0.018 pu
X_{ls}	0.075 pu
X_{lr}	0.12 pu
X_m	3.8 pu
f	50 Hz

REFERENCES

[1] Vries E., 2009. Wind Technology Trends: Why Small Steps Matter,UK Renewable Energy World Magazine.

[2] Lopez J., Sanchis P., Roboam X. and Marroyo L., 2007. Dynamic Behavior of the Doubly Fed Induction Generator During Three Phase Voltage Dip: IEEE Transaction Energy Conversion. 22 (3), 709-717.

[3] Lopez, J., P. Sanchis, X. Roboam and L. Marroyo, 2008. Wind Turbines Based On Doubly Fed Induction Generator Under Asymmetrical Voltage Dips:IEEE Transaction Energy Conversion. 23 (1), 321-330.

[4] Morren J. and S. W. H. de Haan, 2005. Ride Through of Wind Turbines With Doubly-Fed Induction Generator During a voltage Dip: IEEE Transaction Energy Conversion 20 (2),435-441.

[5] Lara O., Z. Liu, G.Q Varela and J.R. McDonald, 2008 Optimal DFIG Crowbar Resistor Design under Different Controllers during Grid Faults: DRPT 6-9 Nanjing China M. Young.

[6] Mortezapour V., H. Lesani and A. Abbaszadeh, 2009. Short Circuit Current Calculation of Doubly Fed Induction Generator: International Conference on Electric Power and Energy Conversion Systems.

[7] Bollen M. H. J., G. Olguin, and M. Martins, 2005. Voltage dips at the terminals of wind power installations: *Wind Energy*, 8, 307–318.

[8] Peng Z. and H. Yikang, 2007 .Control Strategy of an Active Crowbar for DFIG Based Wind Turbine under Grid Voltage Dips: International Conference on Electrical Machines And Systems, Oct. 8~11, Seoul, Korea.

[9] DongY., Y. Xu, H. Li and M. Dai, 2008. Acomparative Study of the Numerical Scales and the Prioritization Methods in AHP: European Journal of Operational Research , 2 (186), 229-242.

[10] AbbaszadehA., s. Lesan and v. Mortezapour, 2009. Transient Response of Doubly Fed Induction Generator under Voltage Sag Using an Accurate Model: Conference on Sustainable Alternative Energy (SAE), IEEE PES/IAS, Valencia.